JOC The Journal of Organic Chemistry

Article

pubs.acs.org/joc

Photoinduced Electron-Transfer-Based Hybridization Probes for Detection of DNA and RNA

Kan Takahashi,[†,⊥] Shun Ito,[§,⊥] Kosuke Nakamoto,[‡] Yasutomo Ito,[∥] and Yoshihito Ueno*[,†,‡]

[†]Course of Applied Life Science, Faculty of Applied Biological Sciences, [‡]United Graduate School of Agricultural Science, and [§]Department of Biomolecular Science, Faculty of Engineering, Gifu University, 1-1 Yanagido, Gifu 501-1193, Japan

[∥]Division for Medical Research Engineering, Nagoya University Graduate School of Medicine, Nagoya 466-8550, Japan

Supporting Information

ABSTRACT: Here, we report the synthesis of a hybridization probe for detection of RNA and DNA based on photoinduced electron transfer (PeT). We designed and synthesized an oligonucleotide containing an adenosine analogue with a 9-(*N*,*N*-dimethylaminomethyl)anthracenyl moiety at its 6-position via an ethynylene linker as the hybridization probe. When the probe was hybridized with a complementary RNA or DNA, the fluorescence intensity increased 3-fold or 4.5-fold, respectively, compared to the single-stranded state.

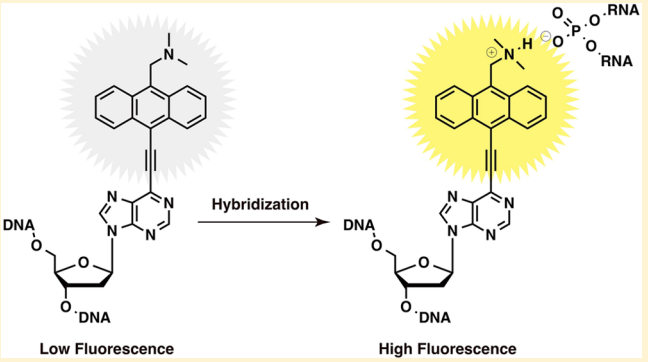

INTRODUCTION

Oligonucleotide (ON) probes modified with fluorescent dyes are widely used to detect specific DNA or RNA molecules.[1,2] Due to the discovery of a large number of noncoding RNAs (ncRNAs),[3] several ON probes modified with a wide variety of dyes have been developed to detect RNAs in living cells.[4−15] For example, a molecular beacon (MB), which is a stem-loop hairpin-structured ON probe, was shown to be able to determine the expression levels of a specific RNA.[4−6] Kool et al. developed the quenched autoligation (QUAL) fluorescence resonance energy transfer (FRET) probe and used it to detect rRNA in mammalian and bacterial cells.[7,8] Okamoto et al. reported an RNA-detecting probe named an exciton-controlled hybridization-sensitive fluorescent ON (ECHO) probe, in which H-aggregation of two thiazole dyes is used to quench their fluorescence.[9−11] Seitz et al. developed an RNA-detecting probe named forced intercalation (FIT) probes containing a thiazole dye as a fluorescent base and, by using it, succeeded in detecting influenza H1N1 mRNA.[12−14]

Recently, we reported the synthesis and properties of fluorescent ON probes containing biaryl analogues.[16−18] We found that these analogues are highly fluorescent, and the incorporation of the analogues into DNA duplexes enhances the thermal and thermodynamic stability of the duplexes.[18] We succeeded in detecting a target RNA using ON probes containing the biaryl analogues.[17,18] As an extension of the study on the synthesis of ONs functionalized with biaryl analogues, here, we designed a hybridization probe, which contained an adenosine analogue **1** with a 9-(*N*,*N*-dimethylaminomethyl)anthracenyl residue at its 6-position via an ethynylene linker, for RNA and DNA detection (Figure 1).

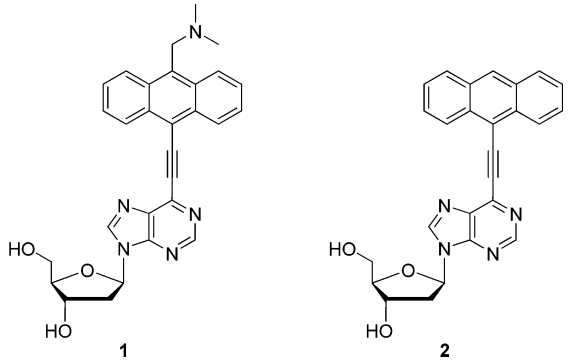

Figure 1. Structures of the 6-modified 2′-deoxyadenosine derivatives.

The mechanism of RNA and DNA detection by this probe is based on photoinduced electron transfer (PeT),[19−21] meaning by quenching of the fluorophore by the amine (Figure 2). We considered that, when the ON probe containing **1** is in a single-stranded state, fluorescence of the anthracene moiety (fluorophore) would be quenched by electron flow from the lone electron pair of the adjacent amine to the empty highest occupied molecular orbital (HOMO). Alternatively, when the ON probe containing **1** forms a duplex with a complementary RNA or DNA, the dimethylamino residue of **1** would be located near the phosphate of the complementary RNA or DNA strand, and this proximity would enhance the protonation of the dimethylamino residue of **1**. The protonation to the

Received: May 21, 2015
Published: August 10, 2015

DOI: 10.1021/acs.joc.5b01132
J. Org. Chem. 2015, 80, 8561−8570

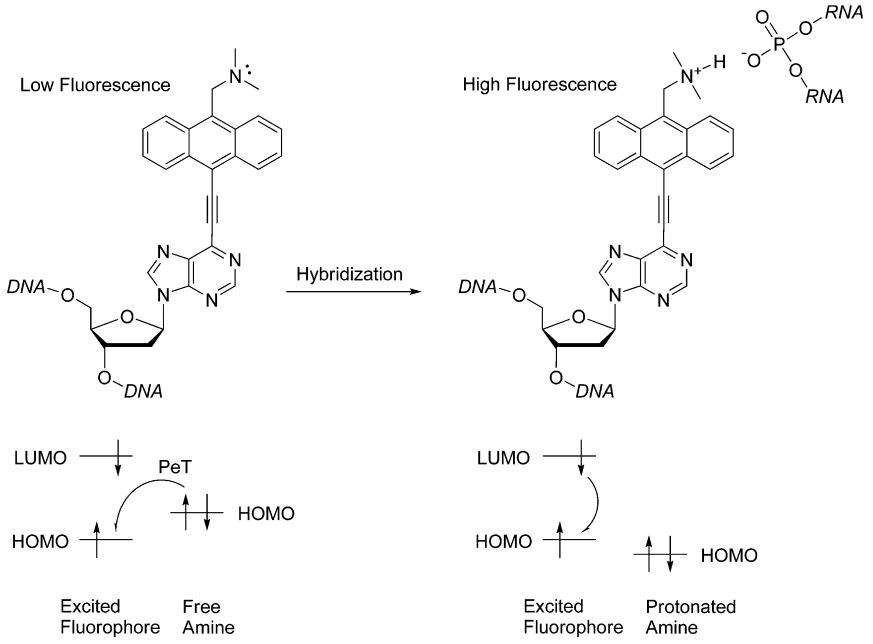

Figure 2. Schematic representation of a PeT-based RNA detection.

Scheme 1

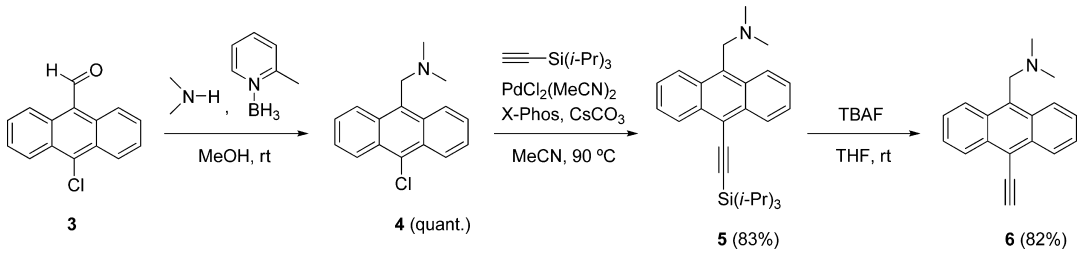

amino residue would lower the HOMO energy level of the amine, leading the ON probe to be more fluorescent. Thus, we expected that the ON probe containing **1** would work as a hybridization probe for RNA and DNA detection.

In this paper, we report the synthesis of an ON probe containing an adenosine analogue **1** with a 9-(*N*,*N*-dimethylaminomethyl)anthracenyl moiety at its 6-position via an ethynylene linker and its ability as a hybridization probe to detect a target RNA and DNA.

RESULTS AND DISCUSSION

Synthesis of Nucleoside Analogues. The synthesis procedure of **1** and the corresponding phosphoramidite unit are shown in Schemes 1 and 3. We also synthesized a fluorescent adenosine analogue **2** without the dimethylamino moiety as a control (Figure 1). First, the synthesis of 9-dimethylaminomethyl-10-chloroanthracene (**4**) was achieved by the reductive amination reaction of 10-chloro-9-anthraldehyde (**3**) with dimethylamine in the presence of 2-picoline borane to give **4**; compound **4** was further coupled with triisopropylacetylene (TIPS-acetylene) in the presence of $PdCl_2(CH_3CN)_2$, 2-dicyclohexylphosphino-2′,4′,6′-triisopropylbiphenyl (X-Phos), and $CsCO_3$ in MeCN at 90 °C to give the ethynyl derivative **5** in 83% yield (Scheme 1). The deprotection of the silyl group using tetra-*n*-butylammonium fluoride (TBAF) afforded the anthracene derivative **6** in 82% yield. In a similar manner, 9-chloroanthracene (**7**) was coupled with TIPS-acetylene to produce the ethynyl derivative **8**; subsequently, **8** was desilylated upon treatment with TBAF to give ethynylanthracene (**9**) in 59% yield (Scheme 2).

Scheme 2

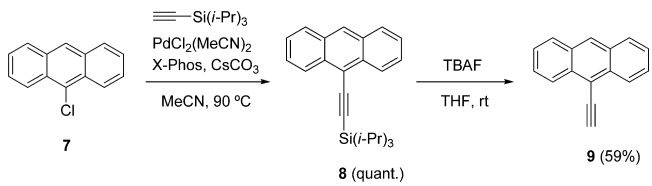

Next, the dimethylaminomethylanthracene derivative **6** was coupled with the 6-iodoadenosine derivative **10**, which was prepared by the reported method, in the presence of $PdCl_2[P(C_6H_5)_3]_2$, CuI, and Et_3N in THF to afford the fluorescent adenosine derivative **11** in 90% yield. Subsequently, **11** was desilylated upon treatment with TBAF to give the fluorescent nucleoside unit **1** (Scheme 3). The primary hydroxy group of **1** was protected by a 4,4′-dimethoxytrityl (DMTr) group to produce a 5′-*O*-DMTr derivative **12**. Compound **12** was phosphitylated by a standard procedure to give the corresponding phosphoramidite **13**. In a similar manner, ethynylanthracene (**9**) was coupled with the 6-iodoadenosine derivative **10** to afford the fluorescent adenosine derivative **14** in 80% yield; subsequently, **14** was desilylated upon treatment

DOI: 10.1021/acs.joc.5b01132
J. Org. Chem. 2015, 80, 8561−8570

Scheme 3

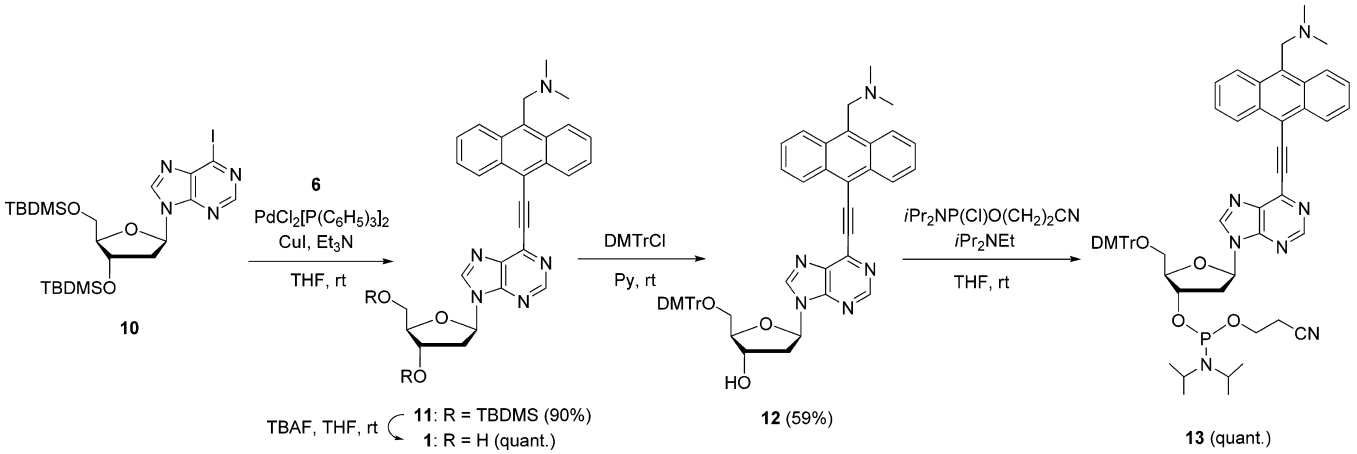

Scheme 4

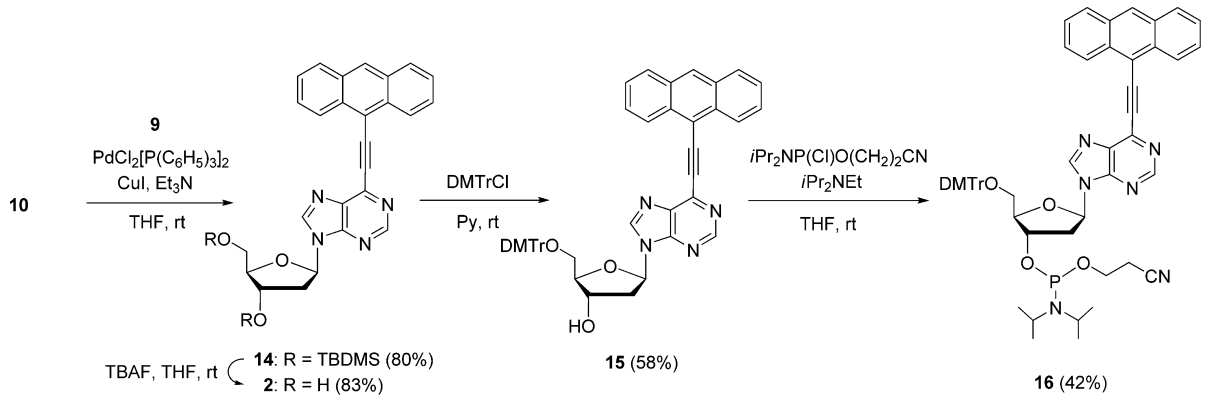

with TBAF to give the fluorescent nucleoside unit **2** (Scheme 4). The primary hydroxy group of **2** was protected by a DMTr group to produce a 5′-*O*-DMTr derivative **15**. Compound **15** was phosphitylated by a standard procedure to give the corresponding phosphoramidite **16**.

Property of Nucleoside Analogues. Before introducing the nucleoside analogues into the oligonucleotides, their photochemical properties were studied. Fluorescence emission spectra of the nucleoside analogue **1** upon excitation at 444 nm in various solvents are shown in Figure 3a. The fluorescence intensity of **1** was dependent on the kind of solvents used: the fluorescence intensity of **1** was greater in H_2O than in other solvents. Fluorescence quantum yields (Φ) of **1** in H_2O, MeOH, EtOAc, THF, and CH_2Cl_2 were 0.111, 0.046, 0.008, 0.009, and 0.010, respectively. Analogue **2** (λ_{ex} = 435 nm) was more fluorescent than **1** (λ_{ex} = 444 nm) in MeOH (Figure 3b). Next, the fluorescence emission intensity of **1** detected at 517 nm upon excitation at 444 nm was measured at various solvent pH values. As shown in Figure 4a, it was found that the fluorescence intensity of **1** was correlated with the pH of the solvent. Analogue **1** became more fluorescent as the pH value decreased. The pK_a of the amino function of **1** was estimated as 7.94 from the pH−fluorescence titration curve. The value was

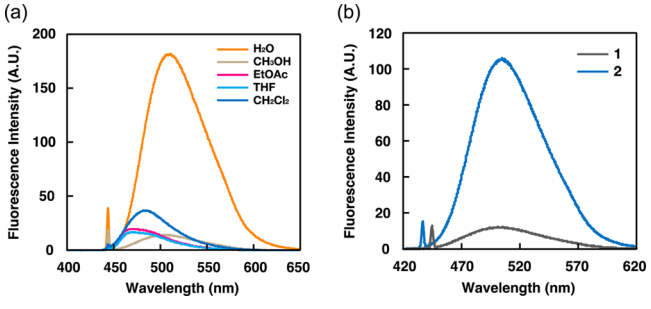

Figure 3. Fluorescence spectra of **1** and **2**. (a) Fluorescence emission spectra of **1** (λ_{ex} = 444 nm, 30 μM **1**) in various solvents at 20 °C and (b) fluorescence emission spectra of **1** (λ_{ex} = 444 nm, 30 μM **1**) and **2** (λ_{ex} = 435 nm, 30 μM **2**) in MeOH at 20 °C. Spectra were recorded using an excitation slit of 1.5 nm and an emission slit of 1.5 nm.

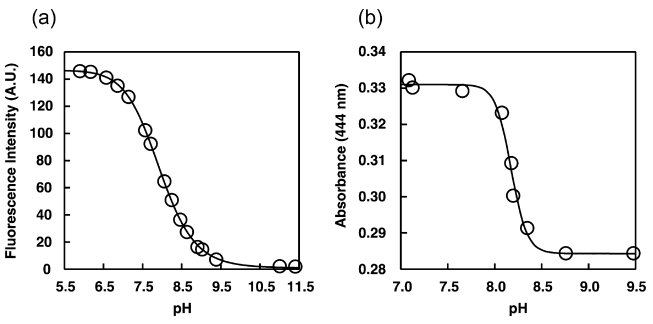

Figure 4. (a) Plots of fluorescence intensity of **1** at 511 nm as a function of pH values (λ_{ex} = 444 nm, 30 μM **1**, 0.1 M Tris-HCl buffer, 20 °C) and (b) plots of absorbance of **1** at 444 nm as a function of pH values (30 μM **1**, 0.1 M Tris-HCl buffer, 20 °C).

DOI: 10.1021/acs.joc.5b01132
J. Org. Chem. 2015, 80, 8561−8570

Table 1. Sequences of Duplexes, ONs, T_m Values of the Duplexes, and Fluorescent Intensities

Abbreviation of duplex	Abbreviation of ON	Sequence[a]	T_m (°C)	ΔT_m (°C)[b]	Fluorescence intensity (A.U.)
Duplex **1**	DNA **3**	5′-d(GAAGGTCATAATATCTCT)-3′			
	DNA **4**	3′-d(CTTCCAGTATTATAGAGA)-5′	51.9	–	–
Duplex **2**	DNA **1**	5′-d(GAAGGTCAT**1**ATATCTCT)-3′			724
	DNA **4**	3′-d(CTTCCAGTATTATAGAGA)-5′	53.6	+1.7	(at 482 nm)
Duplex **3**	DNA **2**	5′-d(GAAGGTCAT**2**ATATCTCT)-3′			334
	DNA **4**	3′-d(CTTCCAGTATTATAGAGA)-5′	50.5	-1.4	(at 510 nm)
Duplex **4**	DNA **3**	5′-d(GAAGGTCATAATATCTCT)-3′			
	DNA **5**	3′-d(CTTCCAGTAATATAGAGA)-5′	44.5	–	–
Duplex **5**	DNA **1**	5′-d(GAAGGTCAT**1**ATATCTCT)-3′			578
	DNA **5**	3′-d(CTTCCAGTAATATAGAGA)-5′	50.7	+6.2	(at 482 nm)
Duplex **6**	DNA **2**	5′-d(GAAGGTCAT**2**ATATCTCT)-3′			317
	DNA **5**	3′-d(CTTCCAGTAATATAGAGA)-5′	51.1	+6.6	(at 510 nm)
Duplex **7**	DNA **3**	5′-d(GAAGGTCATAATATCTCT)-3′			
	DNA **6**	3′-d(CTTCCAGTACTATAGAGA)-5′	43.8	–	–
Duplex **8**	DNA **1**	5′-d(GAAGGTCAT**1**ATATCTCT)-3′			709
	DNA **6**	3′-d(CTTCCAGTACTATAGAGA)-5′	55.3	+11.5	(at 482 nm)
Duplex **9**	DNA **2**	5′-d(GAAGGTCAT**2**ATATCTCT)-3′			357
	DNA **6**	3′-d(CTTCCAGTACTATAGAGA)-5′	52.0	+8.2	(at 510 nm)
Duplex **10**	DNA **3**	5′-d(GAAGGTCATAATATCTCT)-3′			
	DNA **7**	3′-d(CTTCCAGTAGTATAGAGA)-5′	45.7	–	–
Duplex **11**	DNA **1**	5′-d(GAAGGTCAT**1**ATATCTCT)-3′			122
	DNA **7**	3′-d(CTTCCAGTAGTATAGAGA)-5′	53.8	+8.1	(at 482 nm)
Duplex **12**	DNA **2**	5′-d(GAAGGTCAT**2**ATATCTCT)-3′			259
	DNA **7**	3′-d(CTTCCAGTAGTATAGAGA)-5′	51.4	+5.7	(at 510 nm)
Duplex **13**	DNA **3**	5′-d(GAAGGTCATAATATCTCT)-3′			
	RNA **1**	3′-r(CUUCCAGUAUUAUAGAGA)-5′	49.3	–	–
Duplex **14**	DNA **1**	5′-d(GAAGGTCAT**1**ATATCTCT)-3′			631
	RNA **1**	3′-r(CUUCCAGUAUUAUAGAGA)-5′	50.7	+1.4	(at 490 nm)
Duplex **15**	DNA **2**	5′-d(GAAGGTCAT**2**ATATCTCT)-3′			
	RNA **1**	3′-r(CUUCCAGUAUUAUAGAGA)-5′	46.7	–2.6	(at 515 nm)
Duplex **16**	DNA **3**	5′-d(GAAGGTCATAATATCTCT)-3′			
	RNA **2**	3′-r(CUUCCAGUAAUAUAGAGA)-5′	43.6	–	–
Duplex **17**	DNA **1**	5′-d(GAAGGTCAT**1**ATATCTCT)-3′			554
	RNA **2**	3′-r(CUUCCAGUAAUAUAGAGA)-5′	51.0	+7.4	(at 490 nm)
Duplex **18**	DNA **2**	5′-d(GAAGGTCAT**2**ATATCTCT)-3′			
	RNA **2**	3′-r(CUUCCAGUAAUAUAGAGA)-5′	45.4	+1.8	(at 515 nm)
Duplex **19**	DNA **3**	5′-d(GAAGGTCATAATATCTCT)-3′			
	RNA **3**	3′-r(CUUCCAGUACUAUAGAGA)-5′	42.8	–	–
Duplex **20**	DNA **1**	5′-d(GAAGGTCAT**1**ATATCTCT)-3′			612
	RNA **3**	3′-r(CUUCCAGUACUAUAGAGA)-5′	51.6	+8.8	(at 490 nm)
Duplex **21**	DNA **2**	5′-d(GAAGGTCAT**2**ATATCTCT)-3′			
	RNA **3**	3′-r(CUUCCAGUACUAUAGAGA)-5′	46.4	+3.8	(at 515 nm)
Duplex **22**	DNA **3**	5′-d(GAAGGTCATAATATCTCT)-3′			
	RNA **4**	3′-r(CUUCCAGUAGUAUAGAGA)-5′	44.1	–	–
Duplex **23**	DNA **1**	5′-d(GAAGGTCAT**1**ATATCTCT)-3′			224
	RNA **4**	3′-r(CUUCCAGUAGUAUAGAGA)-5′	51.0	+6.9	(at 490 nm)
Duplex **24**	DNA **2**	5′-d(GAAGGTCAT**2**ATATCTCT)-3′			
	RNA **4**	3′-r(CUUCCAGUAGUAUAGAGA)-5′	47.1	+3.0	(at 515 nm)
–	DNA **1**	5′-d(GAAGGTCAT**1**ATATCTCT)-3′	–	–	158 (at 482 nm) 187 (at 490 nm)
–	DNA **2**	5′-d(GAAGGTCAT**2**ATATCTCT)-3′	–	–	181 (at 510 nm) 188 (at 515 nm)

[a]Underlined letters indicate mismatched bases. [b]$\Delta T_m = T_m$ (each duplex) $- T_m$ (Duplexes **1**, **4**, **7**, **10**, **13**, **16**, **19**, or **22**).

almost identical to that (8.16) determined by a pH−UV absorbance titration curve (Figure 4b).

Synthesis of Oligonucleotides. All oligonucleotides were synthesized using a DNA/RNA synthesizer. Sequences of ONs

DOI: 10.1021/acs.joc.5b01132
J. Org. Chem. 2015, 80, 8561−8570

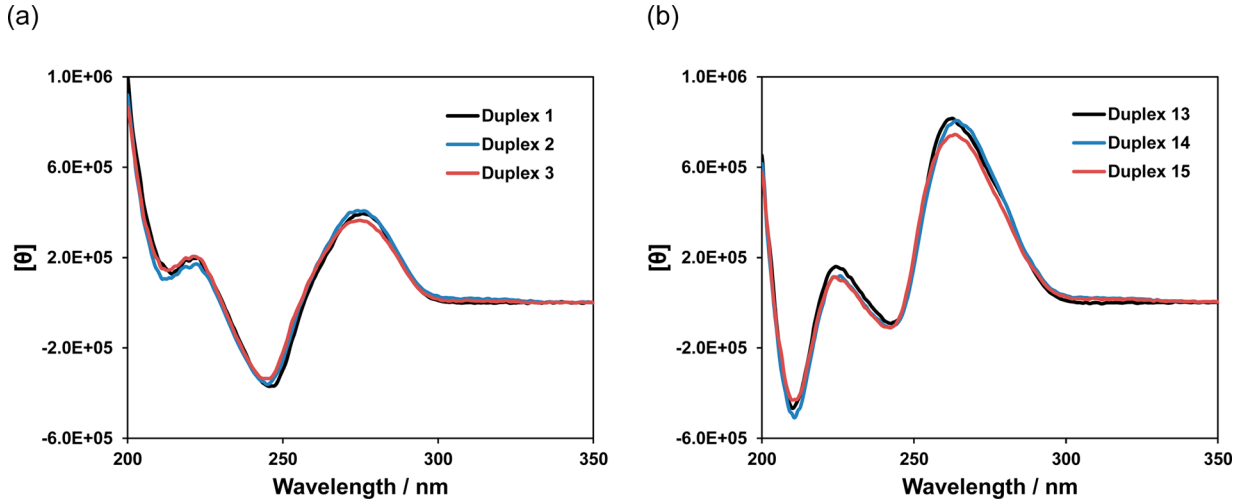

Figure 5. CD spectra of duplexes in a buffer of 10 mM sodium phosphate (pH 7.0) containing 100 mM NaCl at 20 °C: (a) DNA−DNA duplexes and (b) DNA−RNA duplexes. Concentration of duplexes: 30 μM.

used in this study are shown in Table 1. Fully protected ONs (0.2 μmol each), which contained the fluorescent nucleoside analogue **1** or **2**, were treated with concentrated NH_4OH at 55 °C for 12 h. The released ONs were purified using denaturing 20% polyacrylamide gel electrophoresis (PAGE) to yield deprotected ONs. DNA **1** and DNA **2** contained the fluorescent nucleoside analogue **1** or **2** at 12 and 6 OD_{260} absorbance units, respectively. These ONs were analyzed by matrix-assisted laser desorption/ionization time-of-flight mass spectrometry (MALDI-TOF/MS), and the observed molecular weights were in agreement with their structures.

Thermal Stabilities of Duplexes. The thermal stabilities of the DNA/DNA and DNA/RNA duplexes containing analogue **1** or **2** were studied by measuring the melting temperature (T_m) in a buffer containing 10 mM sodium phosphate (pH 7.0) and 100 mM NaCl (Table 1). The T_m value of the complementary DNA/DNA duplex (duplex **1**) between DNA **3** and DNA **4** was 51.9 °C. The T_m of duplex **2** containing analogue **1** was 53.6 °C, while that of duplex **3** containing analogue **2** was 50.5 °C. Thus, it was found that analogue **1**, with the dimethylaminomethylanthracenyl moiety, thermally stabilized the DNA/DNA duplex. Incorporation of a mismatched base pair markedly thermally destabilized the duplex. The T_m values of duplexes **4**, **7**, and **10** with a dA:dA, dA:dC, or dA:dG mismatched base pair were 44.5, 43.8, and 45.7 °C, respectively. On the other hand, the thermal stabilities of the DNA/DNA duplexes containing analogue **1** or **2** seemed to be independent of the type of base opposite the analogues and were not largely different from each other. The T_m values of duplexes **5**, **8**, and **11** with a **1**:dA, **1**:dC, and **1**:dG base pair were 50.7, 55.3, and 53.8 °C, while those of duplexes **6**, **9**, and **12** with a **2**:dA, **2**:dC, and **2**:dG base pair were 51.1, 52.0, and 51.4 °C, respectively. These results suggest that the anthracenylethynyl moieties of analogues **1** and **2** contributed to the thermal stabilization of the duplexes, perhaps by a hydrophobic interaction between the anthracenylethynyl moiety and the adjacent bases. Intriguingly, the T_m values of duplexes **2**, **8**, and **11** with a **1**:dT, **1**:dC, and **1**:dG base pair were greater than those of duplexes **3**, **9**, and **12** with a **2**:dT, **2**:dC, and **2**:dG base pair, respectively. These results suggest that the dimethylaminomethyl moiety of analogue **1** contributes to the thermal stabilization of the duplexes, perhaps by interacting with the phosphates of the complementary strands or the self-strands.

A similar trend was observed for the DNA/RNA duplexes (Table 1). The T_m of the complementary DNA/RNA duplex (duplex **13**) was 51.9 °C, while those of duplexes **16**, **19**, and **22** with a dA:rA, dA:rC, or dA:rG mismatched base pair were 43.6, 42.8, and 44.1 °C, respectively. On the other hand, the T_m values of the duplexes containing analogue **1** were approximately 51 °C, whereas duplexes containing analogue **2** were about 46 °C, irrespective of the type of base opposite the analogues. The T_m values of the duplexes containing **1**:rU, **1**:rA, **1**:rC, or **1**:rG base pairs were greater than those of the duplexes containing **2**:rU, **2**:rA, **2**:rC, or **2**:rG base pairs, respectively. Thus, these results suggest that the dimethylaminomethyl moiety of analogue **1** interacts with the phosphates of the complementary strands or the self-strands also in the DNA/RNA duplexes.

Global Conformations of Duplexes. To investigate the global conformations of the DNA/DNA and DNA/RNA duplexes containing analogue **1** or **2**, circular dichroism (CD) spectra of the duplexes were measured in a buffer of 10 mM sodium phosphate (pH 7.0) and 100 mM NaCl with 30 μM of each duplex (Figure 5). In general, a B-form duplex exhibits a positive CD band around 280 nm and a negative band around 240 nm, while an A-form duplex reveals a positive peak around 270 nm and a negative peak at 210 nm.[22] The shape of the CD spectra of duplexes **2** and **3** with a **1**:dT or **2**:dT base pair was similar to that of the natural DNA duplex **1**. Duplexes **2** and **3** showed positive CD bands around 275 nm and negative bands around 245 nm, which were attributable to the B-form duplex (Figure 5a). The DNA/RNA duplexes **14** and **15** with **1**:rU or **2**:rU base pairs also exhibited CD spectra that were similar to those of the natural DNA/RNA duplex **13**. Duplexes **14** and **15** revealed positive CD bands near 265 nm and negative bands near 210 nm, which were attributable to the A-form duplex (Figure 5b).

Fluorescence Experiments of Duplexes and Single-Stranded DNAs Containing the Analogues. Next, we assessed the ability of DNA **1** and **2** containing either analogue **1** or **2** to detect a target DNA or RNA. Spectra were measured in a buffer containing 10 mM sodium phosphate (pH 7.0) and 100 mM NaCl with 1 μM of each single-stranded DNA or

DOI: 10.1021/acs.joc.5b01132
J. Org. Chem. 2015, 80, 8561−8570

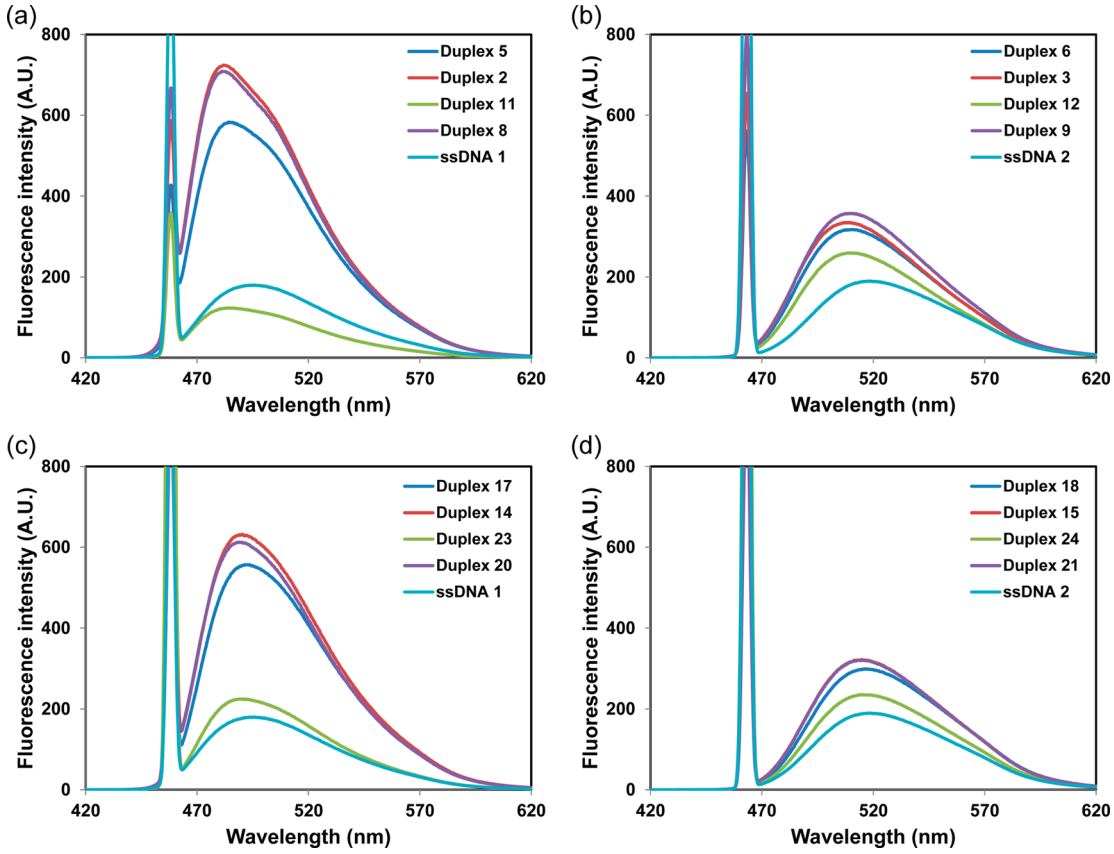

Figure 6. Fluorescence emission spectra of duplexes and single-stranded DNAs containing **1** or **2** in a buffer of 10 mM sodium phosphate (pH 7.0) containing 100 mM NaCl at 20 °C: (a) DNA/DNA duplexes and single-stranded DNA **1** containing **1** (λ_{ex} = 457 nm), (b) DNA/DNA duplexes and single-stranded DNA **2** containing **2** (λ_{ex} = 462 nm), (c) DNA/RNA duplexes and single-stranded DNA **1** containing **1** (λ_{ex} = 457 nm), and (d) DNA/RNA duplexes and single-stranded DNA **2** containing **2** (λ_{ex} = 462 nm). Spectra were recorded using an excitation slit of 3.0 nm and an emission slit of 3.0 nm. Concentration of duplexes and single-stranded DNAs: 1 μM.

duplex. Fluorescence emission spectra (420−620 nm) of the DNA/DNA duplexes are shown in Figure 6a,b. Fluorescence intensities of the duplexes and single-stranded DNA containing analogue **1** (at 482 nm) and of the duplexes and single-stranded DNA containing analogue **2** (at 510 nm) are represented by the bar graph in Figure 7a,b. The fluorescence intensity of the single-stranded DNA (DNA **1**) containing analogue **1** was 158 at 482 nm, while those of the DNA/DNA duplexes with the **1**:dA (duplex **5**), **1**:dT (duplex **2**), **1**:dG (duplex **11**), and **1**:dC (duplex **8**) base pairs were 578, 724, 122, and 709 at 482 nm, respectively. Thus, the duplexes containing the **1**:dA, **1**:dT, and **1**:dC base pairs are more fluorescent than the single-stranded DNA (DNA **1**). It is reported that a guanine base quenches fluorescence of various reporter groups.[23,24] Duplex **11** has a 2′-deoxyguanosine opposite analogue **1**. Thus, duplex **11** might become less fluorescent than the single-stranded DNA (DNA **1**). Duplex **2** with the **1**:dT base pair showed approximately 4.5-fold the fluorescence intensity exhibited by the single-stranded DNA (DNA **1**). On the other hand, the fluorescence intensity of the single-stranded DNA (DNA **2**) containing analogue **2** was 181 at 510 nm, while those of the DNA/DNA duplexes with the **2**:dA (duplex **6**), **2**:dT (duplex **3**), **2**:dG (duplex **12**), and **2**:dC (duplex **9**) base pairs were 317, 334, 259, and 357 at 510 nm, respectively. Thus, the fluorescence intensities of the duplexes are not largely different from those of the single-stranded DNA **2**. These results imply that the DNA with analogue **1** can function as a PeT-based hybridization probe for DNA detection. An alternative explanation for the mechanism of the fluorescence enhancement of the probe is given as follows: The duplex composed of the dimethylaminomethylanthracene-modified probe showed a higher T_m value than that of the anthracene-modified probe. This suggests that dimethylaminomethylanthracene is a better intercalator compared to anthracene. Thus, it was hypothesized that the intercalation of the dimethylaminomethylanthracene moiety might be the cause of the fluorescence enhancement of the probe like ethidium. However, the fluorescence intensity of the dimethylaminomethylanthracene-modified analogue **1** was dependent on the kind of solvents used (Figure 3). The fluorescence intensity of the analogue **1** was greater in H_2O than in other solvents such as CH_3OH, THF, EtOAc, and CH_2Cl_2. Furthermore, the fluorescence intensity of the analogue **1** in CH_3OH was not significantly different from those in less polar solvents such as THF, EtOAc, and CH_2Cl_2. Therefore, these results suggest that the intercalation of the dimethylaminomethylanthracene moiety is not the main cause of the fluorescence enhancement of the probe.

The results for the DNA/RNA duplexes are shown in Figures 6c,d and 7c,d. Similar phenomena were observed for the DNA/RNA duplexes. The fluorescence intensity of the single-stranded DNA (DNA **1**) containing analogue **1** was 177 at 490 nm, while those of the DNA/RNA duplexes with the **1**:rA (duplex **17**), **1**:rU (duplex **14**), **1**:rG (duplex **23**), and **1**:rC (duplex **20**) base pairs were 554, 631, 224, and 612 at 490 nm, respectively. On the other hand, the fluorescence intensity of the single-stranded DNA (DNA **2**) containing analogue **2**

DOI: 10.1021/acs.joc.5b01132
J. Org. Chem. 2015, 80, 8561−8570

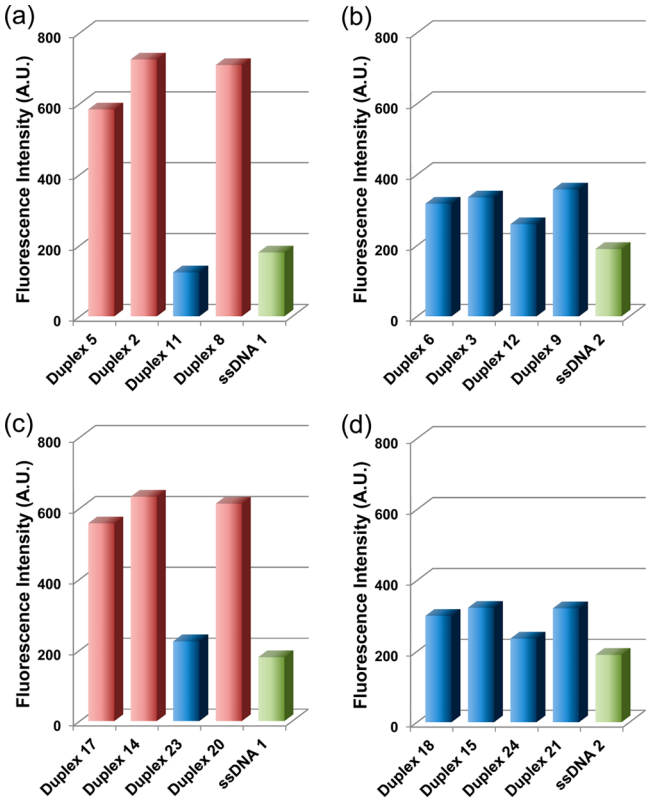

Figure 7. Fluorescence intensity of duplexes and single-stranded DNAs containing **1** or **2**. (a) Fluorescence emission intensity at 482 nm (λ_{ex} = 457 nm). (b) Fluorescence emission intensity at 510 nm (λ_{ex} = 462 nm). (c) Fluorescence emission intensity at 482 nm (λ_{ex} = 457 nm). (d) Fluorescence emission intensity at 510 nm (λ_{ex} = 462 nm). Concentration of duplexes and single-stranded DNAs: 1 μM.

was 188 at 515 nm, while those of the DNA/RNA duplexes with the **2**:rA (duplex **18**), **2**:rU (duplex **15**), **2**:rG (duplex **24**), and **2**:rC (duplex **21**) base pairs were 298, 322, 234, and 320 at 515 nm, respectively. Duplex **14** with the **1**:rU base pair was approximately 3.5 times as fluorescent as the single-stranded DNA (DNA **1**). These results indicate that the DNA with analogue **1** can also work as a PeT-based hybridization probe for RNA detection.

Finally, we examined a photochemical property of the single-stranded DNA **1**. The fluorescence intensity at 493 nm of the single-stranded DNA **1** was monitored upon changing the pH of the buffer. As shown in Figure 8, two transitions were observed around pH 4.0 and 9.0 in the pH−fluorescence profile. The pK_a of the amino function of **1** in the single-stranded DNA **1** was estimated as 4.76 from the pH−fluorescence titration curve from pH 2.5 to 8.5. The value was 3.18 lower than that of the nucleoside monomer **1**. It has been reported that the pK_a of amino groups of some compounds change in a single-stranded DNA due to the change in its microenvironment in the single-stranded state compared to a nucleoside monomer.[25] Based on the results, it was concluded that the amino group of analogue **1** is barely protonated in the single-stranded state in a buffer of pH 7.0. On the other hand, when the DNA formed a duplex with the target RNA or DNA, the dimethylamino group of analogue **1** would be located near the phosphate of the complementary RNA or DNA strand. This proximity would enhance the protonation of the

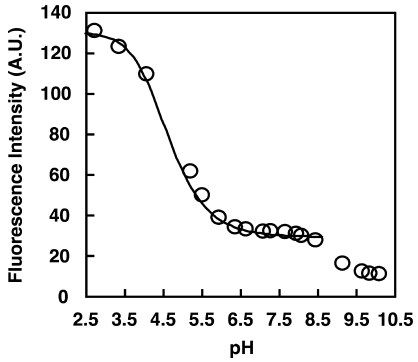

Figure 8. Plots of fluorescence intensity of the single-stranded DNA **1** at 493 nm as a function of pH values (λ_{ex} = 457 nm, 1 μM DNA **1**, 10 mM sodium phosphate, 100 mM NaCl, 20 °C).

dimethylamino residue of analogue **1**, leading the probe to be more fluorescent.

CONCLUSIONS

In conclusion, we have successfully synthesized a PeT-based hybridization probe containing an adenosine analogue **1** with a 9-(*N*,*N*-dimethylaminomethyl)anthracenyl moiety at its 6-position via an ethynylene linker. In addition, duplex **14**, between the probe and the target RNA, which contains the **1**:rU base pair, showed approximately 3.5-fold the fluorescence intensity shown by the single-stranded DNA probe in a buffer of pH 7.0. Duplex **2**, between the probe and the target DNA, which contains the **1**:dT base pair, showed about 4.5-fold the fluorescence intensity exhibited by the single-stranded DNA probe in a buffer of pH 7.0. Therefore, the DNA probe containing analogue **1** may be a promising candidate for a PeT-based hybridization probe to detect target RNA and DNA.

EXPERIMENTAL SECTION

General Remarks. ^{1}H, ^{13}C, and ^{31}P NMR spectra were recorded at 600 and 500 MHz (^{1}H), at 150 and 125 MHz (^{13}C), and at 242 MHz (^{31}P). $CDCl_3$ (CIL) or DMSO-d_6 (CIL) was used as a solvent for obtaining NMR spectra. Chemical shifts (δ) are given in parts per million (ppm) downfield from $(CH_3)_4Si$ (δ 0.00 for ^{1}H NMR in $CDCl_3$), a solvent (δ 39.5 for ^{13}C NMR and δ 2.49 for ^{1}H NMR in DMSO-d_6), or H_3PO_4 (δ 0.00 for ^{31}P NMR in $CDCl_3$) as an internal reference with coupling constants (J) in hertz. The abbreviations s, d, and q signify singlet, doublet, and quartet, respectively. Mass spectra were obtained by electrospray ionization (ESI) time-of-flight (TOF) mass spectrometry. DNA and RNA syntheses were carried out with a DNA/RNA synthesizer. CD spectra were obtained by a circular dichroism spectropolarimeter. Fluorescence emission spectra were obtained by a spectrofluorophotometer. Silica gel chromatography was done with Kanto silica gel 60 N.

9-Dimethylaminomethyl-10-chloroanthracene (4). A mixture of 10-chloro-9-anthraldehyde (0.20 g, 0.83 mmol), dimethylamine (2 M in THF, 0.83 mL), and 2-picoline borane (90 mg, 0.83 mmol) in MeOH (10 mL) was stirred at room temperature for 18 h. The resulting mixture was quenched by using aqueous NH_4Cl (saturated) (2 mL), then partitioned between EtOAc and H_2O. The organic layer was washed with brine, dried (Na_2SO_4), and concentrated. The residue was purified by column chromatography (SiO_2, 25% EtOAc in hexane) to give **4** (0.23 g, 100%): ^{1}H NMR (500 MHz, $CDCl_3$) δ 8.59−8.57 (2H, m), 8.50 (2H, d, J = 8.1), 7.61−7.56 (4H, m), 4.36 (2H, s), 2.37 (6H, s); ^{13}C NMR (125 MHz, DMSO-d_6) δ 131.6, 130.1, 129.4, 128.5, 126.3, 126.0, 125.4, 125.1, 55.3, 45.6; HRMS (ESI-TOF) m/z $[M + H]^+$ calcd for $C_{17}H_{17}ClN$ 270.1050; found 270.1036. Anal. Calcd for $C_{17}H_{16}ClN$: C, 75.69; H, 5.98; N, 5.19. Found: C, 75.58; H, 6.31; N, 4.92.

DOI: 10.1021/acs.joc.5b01132
J. Org. Chem. 2015, 80, 8561−8570

9-Dimethylaminomethyl-10-(triisopropylsilylethynyl)-anthracene (5). A mixture of **3** (1.01 g, 3.70 mmol), $PdCl_2(CH_3CN)_2$ (9.6 mg, 37 μmol), 2-dicyclohexylphosphino-2′,4′,6′-triisopropylbiphenyl (X-Phos) (53 mg, 0.111 mmol), $CsCO_3$ (3.13 g, 9.62 mmol), and TIPS-acetylene (1.01 g, 5.55 mmol) in MeCN (50 mL) was stirred at 90 °C for 24 h. The mixture was partitioned between EtOAc and H_2O. The organic layer was washed with brine, dried (Na_2SO_4), and concentrated. The residue was purified by column chromatography (SiO_2, 10−20% MeOH in $CHCl_3$) to give **5** (1.28 g, 83%): ^{1}H NMR (500 MHz, $CDCl_3$) δ 8.70−8.69 (2H, m), 8.50−8.48 (2H, m), 7.59−7.54 (4H, m), 4.37 (2H, s), 2.36 (6H, s), 1.30−1.26 (21H, m); ^{13}C NMR (125 MHz, $CDCl_3$) δ 132.7, 131.9, 130.8, 127.5, 126.1, 125.9, 125.2, 118.4, 103.6, 103.2, 55.3, 45.6, 18.9, 11.5; HRMS (ESI-TOF) m/z $[M + H]^+$ calcd for $C_{28}H_{38}NSi$ 416.2774; found 416.2770.

9-Dimethylaminomethyl-10-ethynylanthracene (6). To a solution of **5** (0.354 g, 0.852 mmol) in THF (8 mL) was added TBAF (1 M in THF, 1.7 mL), and the mixture was stirred at room temperature for 3 h. The solvent was evaporated in vacuo, and the resulting residue was purified by column chromatography (SiO_2, 20−50% EtOAc in hexane) to give **6** (0.182 g, 82%): ^{1}H NMR (500 MHz, $CDCl_3$) δ 8.66−8.64 (2H, m), 8.52−8.50 (2H, m), 7.60−7.56 (4H, m), 4.38 (2H, s), 4.01 (1H, s), 2.38 (6H, s); ^{13}C NMR (125 MHz, $CDCl_3$) δ 132.8, 132.5, 130.7, 127.3, 126.3, 126.0, 125.2, 116.8, 88.5, 80.6, 55.3, 45.6; HRMS (ESI-TOF) m/z $[M + H]^+$ calcd for $C_{19}H_{18}N$ 260.1439; found 260.1439.

3′,5′-Bis-*O*-(*tert*-butyldimethylsilyl)-6-deamino-2′-deoxy-6-[(10-dimethylaminomethylanthracen-9-yl)ethynyl]adenosine (11). To a mixture of 3′,5′-bis-*O*-(*tert*-butyldimethylsilyl)-6-deamino-2′-deoxy-6-iodoadenosine (**10**) (0.209 g, 0.354 mmol), $PdCl_2[P(C_6H_5)_3]_2$ (20 mg, 28 μmol), CuI (10 mg, 53 μmol), and Et_3N (1.9 mL, 14 μmol) was added a solution of **6** (0.135 g, 0.521 mmol) in THF (5 mL). The reaction mixture was stirred at room temperature for 24 h. The resulting mixture was filtered through a Celite pad, and the eluant was concentrated. The residual oil was dissolved in $CHCl_3$. The organic layer was washed with brine, dried (Na_2SO_4), and concentrated. The residue was purified by column chromatography (SiO_2, 40% EtOAc in hexane) to give **11** (0.230 g, 90%): ^{1}H NMR (500 MHz, $CDCl_3$) δ 9.03 (1H, s), 9.00 (2H, d, J = 8.6), 8.57 (1H, s), 8.54 (2H, d, J = 8.6), 7.68 (2H, t, J = 6.3), 7.62−7.59 (2H, m), 6.58 (1H, t, J = 6.3), 4.69−4.68 (1H, m), 4.41 (2H, s), 4.07−4.06 (1H, m), 3.92 (1H, dd, J = 4.6, 11.5), 3.82 (1H, dd, J = 3.5, 11.5), 2.76−2.71 (1H, m), 2.55−2.50 (1H, m), 2.39 (6H, s), 0.94 (18H, d, J = 4.6), 0.13 (12H, d, J = 4.1); ^{13}C NMR (125 MHz, $CDCl_3$) δ 152.6, 151.0, 143.9, 142.2, 135.4, 134.4, 133.3, 130.7, 127.7, 127.0, 126.3, 125.2, 116.0, 96.3, 95.8, 88.0, 84.5, 71.7, 62.7, 55.4, 45.7, 41.3, 26.0, 18.4, 18.0, −4.7, −4.8, −5.4, −5.5; HRMS (ESI-TOF) m/z $[M + H]^+$ calcd for $C_{41}H_{56}N_5O_3Si_2$ 722.3922; found 722.3923.

6-Deamino-2′-deoxy-6-[(10-dimethylaminomethylanthracen-9-yl)ethynyl]adenosine (1). To a solution of **11** (0.230 g, 0.318 mmol) in THF (5 mL) was added TBAF (1 M in THF, 1.3 mL), and the mixture was stirred at room temperature for 3 h. The solvent was evaporated in vacuo, and the resulting residue was purified by column chromatography (SiO_2, 1−10% MeOH in $CHCl_3$) to give **1** (0.191 g, 100%): ^{1}H NMR (500 MHz, $CDCl_3$) δ 9.01 (1H, s), 8.96 (2H, d, J = 8.7), 8.54 (2H, d, J = 8.7), 8.39 (1H, s), 7.70−7.58 (4H, m), 6.52−6.49 (1H, m), 4.54 (1H, s), 4.41 (2H, s), 4.25 (1H, s), 4.01 (1H, d, J = 13.3), 3.89 (1H, d, J = 13.3), 3.09−3.02 (1H, m), 2.50−2.42 (1H, m), 2.39 (6H, s); ^{13}C NMR (125 MHz, $CDCl_3$) δ 152.9, 150.4, 144.9, 143.0, 136.3, 134.8, 133.3, 130.7, 127.5, 127.2, 126.3, 125.3, 115.6, 97.4, 95.6, 89.4, 87.5, 73.0, 63.2, 55.3, 45.7, 40.9; HRMS (ESI-TOF) m/z $[M + H]^+$ calcd for $C_{29}H_{28}N_5O_3$ 494.2192; found 494.2190.

6-Deamino-2′-deoxy-5′-*O*-(4,4′-dimethoxytrityl)-6-[(10-dimethylaminomethylanthracen-9-yl)ethynyl]adenosine (12). A mixture of **1** (0.136 g, 0.246 mmol) and DMTrCl (0.122 g, 0.359 mmol) in pyridine (5 mL) was stirred at room temoerature. After 3 h, the mixture was partitioned between EtOAc and aqueous $NaHCO_3$ (saturated). The organic layer was washed with brine, dried (Na_2SO_4), and concentrated. The residue was purified by column chromatography (SiO_2, 33−100% EtOAc in hexane) to give **12** (0.130 g, 59%): ^{1}H NMR (600 MHz, $CDCl_3$) δ 8.97 (2H, d, J = 8.9), 8.95 (1H, s), 8.62 (1H, m), 8.54 (2H, d, J = 8.2), 8.35 (1H, s), 7.69−7.67 (2H, m), 7.62−7.59 (2H, m), 7.42−7.41 (2H, m), 7.32−7.27 (7H, m), 6.54 (1H, t, J = 6.9), 4.74−4.73 (1H, m), 4.42 (2H, s), 4.20−4.18 (1H, m), 3.77 (6H, s), 3.48−3.42 (2H, m), 2.95−2.91 (1H, m), 2.63−2.61 (6H, s), 2.39 (6H, s); ^{13}C NMR (150 MHz, $CDCl_3$) δ 158.6, 152.6, 151.0, 149.7, 144.5, 143.9, 142.2, 136.0, 135.6, 135.3, 134.5, 133.2, 130.7, 130.0, 128.1, 127.9, 127.6, 127.1, 127.0, 126.3, 125.3, 123.8, 115.9, 113.2, 96.4, 95.8, 86.6, 86.2, 84.6, 72.4, 63.6, 55.4, 55.2, 45.7, 40.1; HRMS (ESI-TOF) m/z $[M + H]^+$ calcd for $C_{50}H_{46}N_5O_5$ 796.3499; found 796.3519.

3′-*O*-[(2-Cyanoethoxy)(*N*,*N*-diisopropylamino)]phosphanyl-6-deamino-2′-deoxy-5′-*O*-(4,4′-dimethoxytrityl)-6-[(10-dimethylaminomethylanthracen-9-yl)ethynyl]adenosine (13). A mixture of **12** (0.130 g, 0.163 mmol), *N*,*N*-diisopropylethylamine (0.171 mL, 0.978 mmol), and chloro(2-cyanoethoxy)(*N*,*N*-diisopropylamino)phosphine (73 μL, 0.326 mmol) in THF (1 mL) was stirred at room temperature for 1 h. The mixture was partitioned between $CHCl_3$ and aqueous $NaHCO_3$ (saturated). The organic layer was washed with brine, dried (Na_2SO_4), and concentrated. The residue was purified by column chromatography (SiO_2, 50% EtOAc in hexane) to give **13** (0.184 g, 100%): ^{1}H NMR (600 MHz, $CDCl_3$) δ 8.98 (1H, s), 8.96 (2H, d, J = 2.8), 8.54 (d, 2H, J = 8.9), 8.39 (d, 1H, J = 17.2), 7.69−7.67 (2H, m), 7.62−7.59 (2H, m), 7.43−7.41 (2H, m), 7.32−7.30 (4H, m), 7.29−7.27 (2H, m), 7.23−7.20 (1H, m), 6.82−6.79 (4H, m), 6.58−6.55 (1H, m), 4.84−4.79 (1H, m), 4.42 (2H, s), 4.37−4.35 (1H, m), 3.91−3.86 (1H, m), 3.81−3.78 (1H, m), 3.77 (6H, d, J = 3.4), 3.73−3.69 (1H, m), 3.66−3.60 (2H, m), 3.48−3.43 (1H, m), 3.42−3.36 (1H, m), 3.01−2.96 (1H, m), 2.77−2.74 (1H, m), 2.70−2.66 (1H, m), 2.64 (1H, t, J = 6.9), 2.49 (1H, t, J = 6.2), 2.40 (6H, s), 1.30−1.25 (3H, m), 1.22−1.19 (10H, m), 1.14 (3H, d, J = 6.8); ^{31}P NMR (242 MHz, $CDCl_3$) δ 149.7, 149.5; HRMS (ESI-TOF) m/z $[M + H]^+$ calcd for $C_{59}H_{63}N_7O_6P$ 996.4577; found 996.4559.

9-(Triisopropylsilylethynyl)anthracene (8). A mixture of 9-chloroanthracene (**7**) (0.5 g, 2.35 mmol), $PdCl_2(CH_3CN)_2$ (6 mg, 20 μmol), 2-dicyclohexylphosphino-2′,4′,6′-triisopropylbiphenyl (X-Phos) (34 mg, 70 μmol), $CsCO_3$ (2.0 g, 6.1 mmol), and TIPS-acetylene (0.65 g, 3.5 mmol) in MeCN (5 mL) was stirred at 90 °C for 24 h. The mixture was partitioned between EtOAc and H_2O. The organic layer was washed with brine, dried (Na_2SO_4), and concentrated. The residue was purified by column chromatography (SiO_2, hexane) to give **8** (0.70 g, 100%): ^{1}H NMR (500 MHz, $CDCl_3$) δ 8.62 (2H, d, J = 8.6), 8.42 (1H, s), 8.00 (2H, d, J = 8.6), 7.58 (2H, t, J = 8.0), 7.50 (2H, t, J = 7.5), 1.29−1.26 (17H, m), 1.20 (4H, d, J = 7.5); ^{13}C NMR (125 MHz, $CDCl_3$) δ 133.0, 131.1, 128.6, 127.7, 126.8, 126.7, 125.6, 117.6, 19.0, 18.9, 12.1, 11.5; HRMS (ESI-TOF) m/z $[M + H]^+$ calcd for $C_{25}H_{31}Si$ 359.2195; found 359.2174.

9-Ethynylanthracene (9). To a solution of **8** (0.70 g, 3.0 mmol) in THF (5 mL) was added TBAF (1 M in THF, 6 mL), and the mixture was stirred at room temperature for 3 h. The solvent was evaporated in vacuo, and the resulting residue was purified by column chromatography (SiO_2, hexane) to give **9** (0.36 g, 59%): ^{1}H NMR (500 MHz, DMSO-d_6) δ 8.71 (1H, s), 8.45 (2H, d, J = 8.6), 8.16 (2H, d, J = 8.0), 7.69−7.66 (2H, m), 7.59 (2H, t, J = 7.0), 5.17 (1H, s); ^{13}C NMR (125 MHz, $CDCl_3$) δ 133.2, 131.0, 128.7, 128.2, 126.8, 126.5, 125.7, 116.0, 88.2, 80.3; HRMS (ESI-TOF) m/z $[M + H]^+$ calcd for $C_{16}H_{11}$ 203.0861; found 203.0879.

6-(Anthracen-9-yl)ethynyl-3′,5′-bis-*O*-(*tert*-butyldimethylsilyl)-6-deamino-2′-deoxyadenosine (14). To a mixture of **10** (0.57 g, 2.84 mmol), $PdCl_2[P(C_6H_5)_3]_2$ (90 mg, 0.13 mmol), CuI (50 mg, 0.24 mmol), and Et_3N (65 μL, 0.6 mmol) was added a solution of **9** (0.96 g, 1.62 mmol) in THF (10 mL). The reaction mixture was stirred at room temperature for 24 h. The resulting mixture was filtered through a Celite pad, and the eluant was concentrated. The residual oil was dissolved in $CHCl_3$. The organic layer was washed with brine, dried (Na_2SO_4), and concentrated. The residue was purified by column chromatography (SiO_2, 40% EtOAc in hexane) to give **14** (0.86 g, 80%): ^{1}H NMR (500 MHz, $CDCl_3$) δ 9.04 (1H, s), 8.93 (2H, d, J = 8.0), 8.57 (1H, s), 8.55 (1H, s), 8.05 (2H, d, J = 8.6), 7.70−7.67 (2H, m), 7.56 (2H, t, J = 8.0), 6.58 (2H, t, J = 6.3), 4.69−

DOI: 10.1021/acs.joc.5b01132
J. Org. Chem. 2015, 80, 8561−8570

4.68 (1H, m), 4.08−4.07 (1H, m), 3.92 (1H, dd, J = 4.6, 11.5), 3.82 (1H, dd, J = 2.9, 10.9), 2.75−2.71 (1H, m), 2.55−2.52 (1H, m), 0.94 (18H, d, J = 4.6), 0.13 (12H, d, J = 3.5); ^{13}C NMR (125 MHz, $CDCl_3$) δ 152.6, 151.0, 144.0, 142.1, 135.3, 133.6, 131.0, 130.0, 128.7, 127.5, 127.0, 125.9, 115.2, 96.0, 95.5, 88.0, 84.5, 71.7, 62.7, 41.3, 26.0, 25.8, 18.5, 18.0, −4.7, −4.8, −5.4, −5.5; HRMS (ESI-TOF) m/z [M + H]$^+$ calcd for $C_{38}H_{49}N_4O_3Si_2$ 665.3343; found 665.3352.

6-(Anthracen-9-yl)ethynyl-6-deamino-2′-deoxyadenosine (2). To a solution of **14** (0.86 g, 1.30 mmol) in THF (10 mL) was added TBAF (1 M in THF, 2.6 mL), and the mixture was stirred at room temperature for 3 h. The solvent was evaporated in vacuo, and the resulting residue was purified by column chromatography (SiO_2, 0−10% MeOH in $CHCl_3$) to give **2** (0.48 g, 83%): ^{1}H NMR (500 MHz, DMSO-d_6) δ 9.01 (2H, d, J = 13.8), 8.86 (1H, s), 8.75 (2H, d, J = 8.6), 8.23 (2H, d, J = 8.1), 7.81 (2H, t, J = 6.9) 7.66 (2H, t, J = 7.5), 6.54 (1H, t, J = 6.3), 5.40 (1H, d, J = 4.0), 5.02 (1H, t, J = 5.2), 4.50−4.48 (1H, m), 3.94−3.93 (1H, m), 3.69−3.64 (1H, m), 3.60−3.55 (1H, m), 2.86−2.81 (1H, m), 2.44−2.40 (1H, m); ^{13}C NMR (125 MHz, DMSO-d_6) δ 152.2, 151.1, 146.0, 140.2, 134.7, 132.7, 130.6, 129.2, 128.3, 126.3, 125.6, 113.7, 95.8, 93.8, 88.1, 83.9, 70.5, 61.5; HRMS (ESI-TOF) m/z [M + H]$^+$ calcd for $C_{26}H_{21}N_4O_3$ 437.1614; found 437.1590.

6-(Anthracen-9-yl)ethynyl-6-deamino-2′-deoxy-5′-*O*-(4,4′-dimethoxytrityl)adenosine (15). A mixture of **2** (0.48 g, 1.09 mmol) and DMTrCl (0.44 g, 1.30 mmol) in pyridine (5 mL) was stirred at room temperature. After 3 h, the mixture was partitioned between EtOAc and aqueous $NaHCO_3$ (saturated). The organic layer was washed with brine, dried (Na_2SO_4), and concentrated. The residue was purified by column chromatography (SiO_2, 0−66% EtOAc in hexane) to give **15** (0.43 g, 58%): ^{1}H NMR (600 MHz, $CDCl_3$) δ 8.96 (1H, s), 8.91 (2H, d, J = 8.9), 8.56 (1H, s), 8.35 (1H, s), 8.05 (2H, d, J = 8.2), 7.70−7.68 (2H, m), 7.56 (2H, t, J = 7.6), 7.42 (2H, d, J = 7.6), 7.32−7.27 (6H, m), 7.24−7.21 (1H, m), 6.83−6.81 (4H, m), 6.55 (1H, t, J = 6.2), 4.75−4.74 (1H, m), 4.19 (1H, q, J = 4.1), 3.77 (6H, s), 3.48−3.42 (2H, m), 2.97−2.92 (1H, m), 2.64−2.60 (1H, m), 2.05 (1H, s); ^{13}C NMR (150 MHz, $CDCl_3$) δ 158.6, 152.6, 151.0, 144.5, 143.9, 142.2, 135.6, 135.3, 133.6, 131.0, 130.1, 130.0, 128.7, 128.1, 127.9, 127.6, 127.0, 126.9, 126.0, 115.0, 113.2, 96.1, 95.4, 86.7, 86.2, 84.6, 72.5, 63.6, 55.2, 40.1; HRMS (ESI-TOF) m/z [M + H]$^+$ calcd for $C_{47}H_{39}N_4O_5$ 739.2920; found 739.2922.

6-(Anthracen-9-yl)ethynyl-3′-*O*-[(2-cyanoethoxy)(*N*,*N*-diisopropylamino)]phosphanyl-6-deamino-2′-deoxy-5′-*O*-(4,4′-dimethoxytrityl)adenosine (16). A mixture of **15** (0.29 g, 0.40 mmol), *N*,*N*-diisopropylethylamine (0.42 mL, 2.38 mmol), and chloro(2-cyanoethoxy)(*N*,*N*-diisopropylamino)phosphine (0.18 mL, 0.79 mmol) in THF (2 mL) was stirred at room temperature for 1 h. The mixture was partitioned between $CHCl_3$ and aqueous $NaHCO_3$ (saturated). The organic layer was washed with brine, dried (Na_2SO_4), and concentrated. The residue was purified by column chromatography (SiO_2, 50% EtOAc in hexane) to give **16** (0.16 g, 42%): ^{1}H NMR (600 MHz, $CDCl_3$) δ 8.97 (1H, d, J = 3.0), 8.91 (2H, d, J = 8.2), 8.56 (1H, s), 8.40 (1H, d, J = 16.5), 8.05 (2H, d, J = 8.2), 7.69 (2H, t, J = 6.8), 7.56 (2H, t, J = 7.6), 7.42 (2H, t, J = 5.5), 7.33−7.30 (4H, m), 7.29−7.28 (2H, m), 7.23−7.21 (1H, m), 6.82−6.77 (4H, m), 6.58−6.55 (1H, m), 4.82 (1H, m), 4.37−4.35 (1H, m), 3.88−3.87 (1H, m), 3.77 (6H, d, J = 3.4), 3.73−3.69 (1H, m), 3.65−3.61 (2H, m), 3.49 (1H, s), 3.47−3.42 (1H, m), 3.40−3.36 (1H, m), 3.01−2.97 (1H, m), 2.81−2.78 (1H, m), 2.69 (1H, m), 2.64 (1H, t, J = 6.2), 2.49 (1H, t, J = 6.8), 1.32−1.29 (3H, m), 1.27−1.25 (3H, m), 1.20−1.19 (3H, m), 1.14 (3H, d, J = 6.9); ^{31}P NMR (242 MHz, $CDCl_3$) δ 149.6, 149.5; HRMS (ESI-TOF) m/z [M + H]$^+$ calcd for $C_{38}H_{49}N_4O_3Si_2$ 665.3343; found 665.3352.

ON Synthesis. Synthesis was carried out with a DNA/RNA synthesizer by a phosphoramidite method. Deprotection and purification of DNAs: Deprotection of bases and phosphates was performed in concentrated NH_4OH at 55 °C for 16 h. The oligonucleotides were purified by 20% PAGE containing 7 M urea to give the highly purified DNA **1** (12), DNA **2** (6), DNA **3** (26), DNA **4** (14), DNA **5** (18), DNA **6** (17), and DNA **7** (49). Deprotection and purification of RNAs: Deprotection of bases and phosphates was performed in concentrated NH_4OH/EtOH (3:1, v/v) at 55 °C for 4 h. 2′-*O*-TBDMS groups were removed by $Et_3N{\cdot}3HF$ (125 μL) in DMSO (100 μL) at 65 °C for 90 min. The reaction was quenched with 0.1 M triethylammonium acetate buffer (pH 7.0) and desalted on a Sep-Pak C18 cartridge. Deprotected RNAs were purified by 20% PAGE containing 7 M urea to give the highly purified RNA **1** (10), RNA **2** (13), RNA **3** (8), RNA **4** (14). The yields are indicated in parentheses as OD units at 260 nm starting from 0.2 μmol scale.

MALDI-TOF/MS Analysis of ONs. Spectra were obtained with a time-of-flight mass spectrometer equipped with a nitrogen laser (337 nm, 3 ns pulse). A solution of 3-hydroxypicolinic acid and diammonium hydrogen citrate in H_2O was used as the matrix. Data of synthetic ONs: DNA **1** m/z = 5738.7 ([M − H]$^-$, calcd 5738.9; $C_{196}H_{237}N_{66}O_{106}P_{17}$); DNA **2** m/z = 5682.5 ([M − H]$^-$, calcd 5681.8; $C_{193}H_{230}N_{65}O_{106}P_{17}$); DNA **3** m/z = 5497.2 ([M − H]$^-$, calcd 5496.6; $C_{177}H_{223}N_{66}O_{106}P_{17}$); DNA **4** m/z = 5501.2 ([M − H]$^-$, calcd 5496.6; $C_{177}H_{223}N_{66}O_{106}P_{17}$); DNA **5** m/z = 5505.6 ([M − H]$^-$, calcd 5505.6; $C_{177}H_{222}N_{69}O_{104}P_{17}$); DNA **6** m/z = 5485.1 ([M − H]$^-$, calcd 5481.6; $C_{176}H_{222}N_{67}O_{105}P_{17}$); DNA **7** m/z = 5522.1 ([M − H]$^-$, calcd 5521.6; $C_{177}H_{222}N_{69}O_{105}P_{17}$); RNA **1** m/z = 5704.0 ([M − H]$^-$, calcd 5700.4; $C_{171}H_{210}N_{66}O_{124}P_{17}$); RNA **2** m/z = 5727.8 ([M − H]$^-$, calcd 5723.5; $C_{172}H_{212}N_{69}O_{122}P_{17}$); RNA **3** m/z = 5702.2 ([M − H]$^-$, calcd 5699.4; $C_{171}H_{212}N_{67}O_{123}P_{17}$); RNA **4** m/z = 5742.4 ([M − H]$^-$, calcd 5739.5; $C_{172}H_{212}N_{69}O_{123}P_{17}$).

Thermal Denaturation Study. The solution containing the duplex in a buffer composed of 10 mM sodium phosphate (pH 7.0) and 0.1 M NaCl was heated at 95 °C for 3 min, cooled gradually to an appropriate temperature, and then used for the thermal denaturation study. The thermal-induced transition of each mixture was monitored at 260 nm on UV−vis spectrophotometer fitted with a temperature controller in quartz cuvettes with a path length of 1.0 cm and a 3.0 μM duplex concentration in a buffer of 10 mM sodium phosphate (pH 7.0) and 0.1 M NaCl. The sample temperature was increased by 0.5 °C/min.

CD Spectroscopy. CD spectra were measured by a spectropolarimeter. The samples for CD spectroscopy were prepared by the same procedure used in the thermal denaturation study with a 30 μM duplex concentration, and spectra were recorded at 20 °C. The molar ellipticity was calculated from the following equation: $[\theta] = \theta/cL$, where θ is the relative intensity, c is the sample concentration, and L is the cell path length in centimeters.

Fluorescence Experiments. Fluorescence emission spectra were obtained on a spectrofluorophotometer in quartz cuvettes with a path length of 1.0 cm and a 30 μM nucleoside analogue concentration in various solvents or a 3.0 μM duplex or single-stranded DNA concentration in a buffer of 10 mM sodium phosphate (pH 7.0) containing 100 mM NaCl at 20 °C. Spectra were recorded with use of an excitation slit of 1.5 nm and an emission slit of 1.5 nm for nucleoside monomer or use of an excitation slit of 3.0 nm and an emission slit of 3.0 nm for duplex or single-stranded DNA. The fluorescence quantum yield (Φ_{em}) was determined by use of quinine as a reference with the known Φ_{em} value of 0.58 (22 °C) in 0.1 M H_2SO_4. The quantum yield was calculated according to the following equation:[26] $\Phi_{em(S)}/\Phi_{em(R)} = (I_{(S)}/I_{(R)}) \times (A_{(R)}/A_{(S)}) \times (n_{(S)}^2/n_{(R)}^2)$. Here, $\Phi_{em(S)}$ and $\Phi_{em(R)}$ are the fluorescence quantum yields of the sample and the reference, respectively, $I_{(S)}$ and $I_{(R)}$ are the integrated fluorescence intensities of the sample and the reference, respectively, $A_{(S)}$ and $A_{(R)}$ are the respective optical density of the sample and the reference solutions at the wavelength of excitation, and $n_{(S)}^2$ and $n_{(R)}^2$ are the values of the refractive index for the respective solvents.

Titration Experiments. The pK_a values were determined from the fluorescence intensity or absorbance of the samples at 20 °C. A 30 μM solution of the nucleoside analogue **1** in 100 mM Tris-HCl buffer or a 3 μM solution of the single-stranded DNA **1** in 10 mM sodium phosphate buffer containing 100 mM NaCl was used. The pH was adjusted by adding small amounts of concentrated NaOH solution to the samples.

DOI: 10.1021/acs.joc.5b01132
J. Org. Chem. 2015, 80, 8561−8570

■ ASSOCIATED CONTENT

Supporting Information

The Supporting Information is available free of charge on the ACS Publications website at DOI: 10.1021/acs.joc.5b01132.

^{1}H NMR spectra of compounds **1**, **2**, **4**−**6**, **8**, **9**, **11**−**16**. ^{13}C NMR spectra of compounds **1**,**2**, **4**−**6**, **8**, **9**, **11**, **12**, **14**, and **15**. ^{31}P NMR spectra of compounds **13** and **16**. Profiles of the melting curves of the duplexes (PDF)

■ AUTHOR INFORMATION

Corresponding Author

*Phone: +81-58-293-2919. Fax: +81-58-293-2919. E-mail: uenoy@gifu-u.ac.jp.

Author Contributions

⊥K.T. and S.I. contributed equally to this work.

Notes

The authors declare no competing financial interest.

■ ACKNOWLEDGMENTS

This research was partially supported by the Ministry of Education, Culture, Sports, Science, and Technology in Japan [Grant-in-Aid for Exploratory Research 24659045] and the C19 Kiyomi Yoshizaki research grant.

■ REFERENCES

(1) Malinovskii, V. L.; Wenger, D.; Häner, R. *Chem. Soc. Rev.* **2010**, *39*, 410−422.
(2) Preus, S.; Wilhelmsson, L. M. *ChemBioChem* **2012**, *13*, 1990−2001.
(3) He, L.; Hannon, G. J. *Nat. Rev. Genet.* **2004**, *5*, 522−531.
(4) Santangelo, P. J.; Nix, B.; Tsourkas, A.; Bao, G. *Nucleic Acids Res.* **2004**, *32*, e57.
(5) Wang, K.; Tang, Z.; Yang, C. J.; Kim, Y.; Fang, X.; Li, W.; Wu, Y.; Medley, C. D.; Cao, Z.; Li, J.; Colon, P.; Lin, H.; Tan, W. *Angew. Chem., Int. Ed.* **2009**, *48*, 856−870.
(6) Monroy-Contreras, R.; Vaca, L. *J. Nucleic Acids* **2011**, *2011*, 1.
(7) Sando, S.; Kool, E. T. *J. Am. Chem. Soc.* **2002**, *124*, 9686−9687.
(8) Abe, H.; Kool, E. T. *Proc. Natl. Acad. Sci. U. S. A.* **2006**, *103*, 263−268.
(9) Okamoto, A.; Sugizaki, K.; Yuki, M.; Yanagisawa, H.; Ikeda, S.; Sueoka, T.; Hayashi, G.; Wang, D. O. *Org. Biomol. Chem.* **2013**, *11*, 362−371.
(10) Kubota, T.; Ikeda, S.; Yanagisawa, H.; Yuki, M.; Okamoto, A. *PLoS One* **2010**, *5*, e13003.
(11) Hayashi, G.; Okamoto, A. *Chem. Rec.* **2013**, *13*, 209−217.
(12) Kummer, S.; Knoll, A.; Socher, E.; Bethge, L.; Herrmann, A.; Seitz, O. *Angew. Chem., Int. Ed.* **2011**, *50*, 1931−1934.
(13) Kummer, S.; Knoll, A.; Socher, E.; Bethge, L.; Herrmann, A.; Seitz, O. *Bioconjugate Chem.* **2012**, *23*, 2051−2060.
(14) Hövelmann, F.; Gaspar, I.; Ephrussi, A.; Seitz, O. *J. Am. Chem. Soc.* **2013**, *135*, 19025−19032.
(15) Asanuma, H.; Akahane, M.; Niwa, R.; Kashida, H.; Kamiya, Y. *Angew. Chem., Int. Ed.* **2015**, *54*, 4315−4319.
(16) Ueno, Y.; Kato, T.; Sato, K.; Ito, Y.; Yoshida, M.; Inoue, T.; Shibata, A.; Ebihara, M.; Kitade, Y. *J. Org. Chem.* **2005**, *70*, 7925−7935.
(17) Ueno, Y.; Kawamura, A.; Takasu, K.; Komatsuzaki, S.; Kato, K.; Kuboe, S.; Kitamura, Y.; Kitade, Y. *Org. Biomol. Chem.* **2009**, *7*, 2761−2769.
(18) Ueno, Y.; Komatsuzaki, S.; Takasu, K.; Kawai, S.; Kitamura, Y.; Kitade, Y. *Eur. J. Org. Chem.* **2009**, *28*, 4763−4769.
(19) Lakowicz, J. R. *Principles of Fluorescence Spectroscopy*, 3rd ed.; Springer: New York, 2006; pp 641−643.
(20) Bryan, A. J.; de Silva, A. P.; de Silva, S. A.; Rupasinghe, R. A. D. D.; Sandanayake, K. R. A. S. *Biosensors* **1989**, *4*, 169−179.
(21) Huston, M. E.; Akkaya, E. U.; Czarnik, A. W. *J. Am. Chem. Soc.* **1989**, *111*, 8735−8737.
(22) Bloomfield, V. A.; Crothers, D. M.; Tinoco, I., Jr. *Nucleic Acids: Structure, Properties, and Functions*; University Science Books: Sausalito, CA, 2000; pp 185−199.
(23) Heinlein, T.; Knemeyer, J. P.; Piestert, O.; Sauer, M. *J. Phys. Chem. B* **2003**, *107*, 7957−7964.
(24) Venkatesan, N.; Seo, Y. J.; Kim, B. H. *Chem. Soc. Rev.* **2008**, *37*, 648−663.
(25) Kashida, H.; Sano, K.; Hara, Y.; Asanuma, H. *Bioconjugate Chem.* **2009**, *20*, 258−265.
(26) Lakowicz, J. R. *Principles of Fluorescence Spectroscopy*, 3rd ed.; Springer: New York, 2006; pp 54−55.

DOI: 10.1021/acs.joc.5b01132
J. Org. Chem. 2015, 80, 8561−8570